

# Modeling specifications for HiVision Millimeter Wave Radar for multisensory Enhanced Vision Systems

Devendran.B<sup>\*</sup>, Dr.Sudesh Kumar Kashyap<sup>\*\*</sup>, Dr.T.V.Rama Murthy<sup>\*\*\*</sup>

<sup>\*</sup> Student (M-tech in signal processing), REVA Institute of Technology and Management, Bangalore, yashudevendran@gmail.com

<sup>\*\*</sup> Principal Scientist, FMCD, CSIR-National Aerospace Laboratories, Bangalore, India, sudesh@nal.res.in

<sup>\*\*\*</sup> Senior professor, Dept. of Electronics and Communication Engineering, REVA Institute of Technology and Management, Bangalore, drtvramamurthy@revainstitution.org

**Abstract** – A number of projects have been developed to increase flight safety and economy of aviation. The development and validation of systems for pilot assistance is also one field of interest. To improve the situational awareness of an aircrew during poor visibility, different approaches emerged during the past few years. Enhanced vision systems (EVS – based on sensor images) are one of those. Typically, Enhanced vision systems consist of two main parts- sensor vision and Synthetic vision. Sensor vision uses weather penetrating forward looking image sensors such as Forward Looking Infrared Radar (FLIR) and HiVision Millimeter Wave Radar (HiVision MMWR). The main contribution of this paper is to set up the procedure based on literature survey to model the HiVision Millimeter Wave Radar for Enhanced Vision Systems functionalities.

**Key words** - Enhanced Vision Systems (EVS), Millimeter Wave Radar (MMWR), and Phong like lighting model, Normalized Radar Cross Section (NRCS).

## I. INTRODUCTION

Enhanced vision systems technology is a combination of synthetic vision and sensor vision. Synthetic vision relies on onboard terrain databases and navigation data. Although the synthetic images are clearly understandable for the pilot they suffer from poor reliability. On the other hand, sensor vision referencing the real time situations and acquiring images by using forward looking imaging sensors that can penetrate darkness and weather phenomena (such as fog and haze). They provide means for the pilot to obtain the necessary "visual" cues. Sensors are either passive (as in the case of Forward Looking Infra-Red or FLIR), or active (as in the case of Milli Meter Wave Radar or MMWR) [1]. The additional use of forward looking imaging sensors offers the possibility to detect unexpected obstacles, the monitoring of the integrity of databases and navigation data and the extraction of navigation information, e.g. the relative position of runway and aircraft, directly from the sensor data. Typical Enhanced vision Systems concept is shown in fig.1

The performance of the Enhanced Vision System relies on the performance of imaging sensors. Designing an imaging sensor that is accurate and operational in real-time is a significant challenge. If EVS technology is mainly justified by an increase of the crew's (visual) situation awareness under adverse weather conditions the all-weather capabilities of the sensors will become the most important characteristic. From this point of view the UV, the MMW and the PMMW sensor should be taken into account. The UV sensor and the passive

MMW sensor need some additional ground facilities (UV-sources and MMW reflectors), the first one in general and the latter one in adverse weather conditions. Additional ground facilities might be no problem, especially if they are cheap and easy to install, but they restrict the EVS technology to certain scenarios with a ground based infra-structure, which might be not always available. Hence, among all the imaging sensors, the most promising one for Enhanced Vision System is the imaging millimeter wave radar. Because millimeter wave radar has the lowest weather dependency. To avoid the drawbacks of sensor vision and synthetic vision technologies and to maintain the benefits of both, it is necessary to fuse them into a single system called Enhanced Vision Systems (EVS) [2, 4].

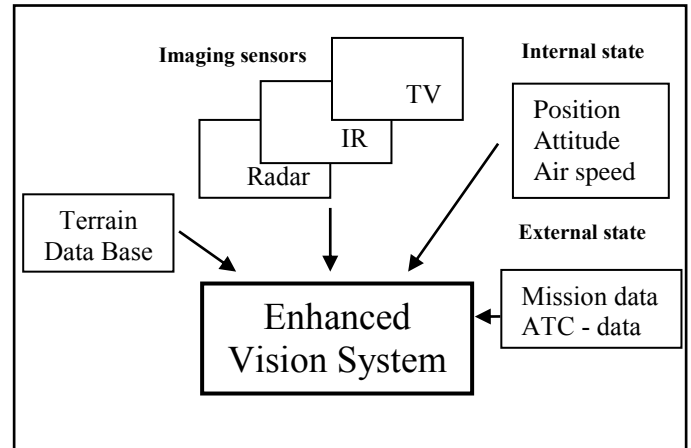


Fig.1. Typical Enhanced Vision System concept

In this paper details are presented on the millimeter wave radar modeling procedures, and modeling parameters. No previous publications have collected all the information required for radar modeling. However, the authors have attempted to present complete specifications required for radar modeling.

## II. HIVISION MILLIMETER WAVE RADAR MODELING

### Major requirements of EVS sensor selection

For adequate enhanced vision sensors, there exist at least three major requirements:

- Weather independence and board autonomy

Sensor data should not be influenced by different weather conditions and sensor data acquisition should be done with as few ground equipment as possible.

- Frame rate

Sensor data should be available with a frame rate of 16 Hz or higher to provide persistence of vision.

- Extraction of needed information

Either the aircrew or a machine vision system should be able to extract the information out of sensor data needed to perform a given task, e.g. landing under adverse weather conditions [3].

As seen from the table.1, HiVision radar seems to be the most sophisticated enhanced vision sensor with reference to first two requirements mentioned above; in the later part third requirement will be discussed in detail.

Sensor	Imaging Principle	Image rate[Hz]	Resolution	Visual Range
IR	optical	25	0.05	?
LADAR	2.5-D	2	0.35 <sup>0</sup> x0.20 <sup>0</sup> 1m	400?
UV	optical	25	0.05 <sup>0</sup>	>800
MMW radar (HiVision)	Angle/range	16	0.25 <sup>0</sup> 6m	>3000
MMW radar pencil beam	2.5D	<1	2.5 <sup>0</sup>	>3000
PMMW spectrometer	optical	17	0.5 <sup>0</sup>	700

Table 1: characteristics of potential EVS sensor (see [4] for more detailed overview)

- UV = Ultra Violet
- LADAR - LAsEr raDAR
- IR - Infra Red
- MMW - MilliMeter Wave radar
- PBMMW - Pencil Beam MilliMeter Wave radar
- PMMW - Passive MilliMeter Wave sensor

### Selection of the transmitting frequency

There are two frequencies suitable for the observation of extreme weather conditions such as fog and cloud by radar, 35 and 94 GHz. At 94 GHz, a drop's backscatter cross section is larger, by about 17 dB, than that at 35 GHz. However, a peak transmitting power of about 100 kW is available at 35 GHz, whereas the peak power is only a few kilowatts at 94 GHz. This difference of more than 18 dB cancels the larger cross section at 94 GHz. In addition, a 94-GHz radar has other disadvantages for ground based applications: larger attenuation by the atmosphere, larger loss in the waveguide components, and a relatively high noise figure for the receiver, when compared with a 35-GHz radar. In a vertically pointing mode, the attenuation by the atmosphere is relatively small compared to that on longer horizontal paths near the ground. Therefore, a 94-GHz radar is best suited for vertical observation in airborne or satellite-borne applications, wherein it is important to decrease size and weight. On the other hand, a 35-GHz radar is best suited for ground based observations. Since EVS is ground based application, 35-GHz frequency is selected as a center frequency for MMW radar. Figure 2 supports the above discussion.

### Image processing

Figure 3 shows the imaging geometry for MMW radar. From figure we can make out that the radar looking

down towards the ground and makes the angle  $\theta_0$  with respect to ground, which is assumed flat and horizontal.

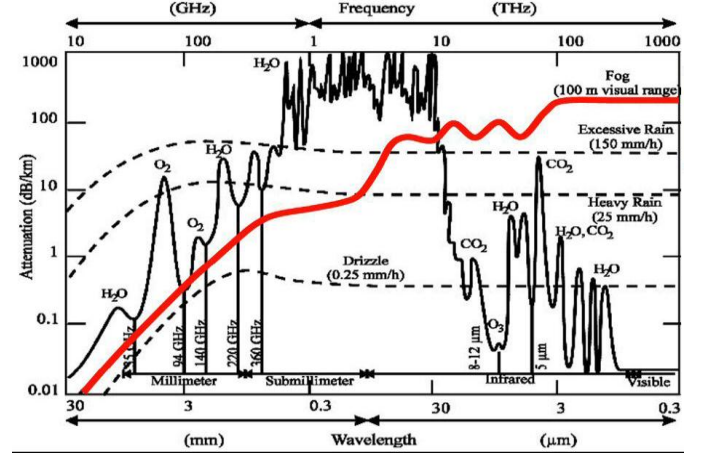


Fig.2. Attenuation of the atmosphere (in dB/km) for different visual conditions is depending on wavelength [5]

The sweep angle  $\varphi = 0$  makes an angle  $\theta_0$  in viewing direction and more generally, an angle  $\theta_\varphi = \theta(\varphi)$  for an arbitrary sweep angle  $\varphi$ . The other important parameter is range R, which is measured by using Doppler principle. The antenna beam is assumed to be a vertical fan with a 3dB width of  $\varphi_{3dB}$  [rad]. Hence for each sweep angle  $\varphi$ , the antenna footprint on the ground is a wedge shown by strips in figure 3.

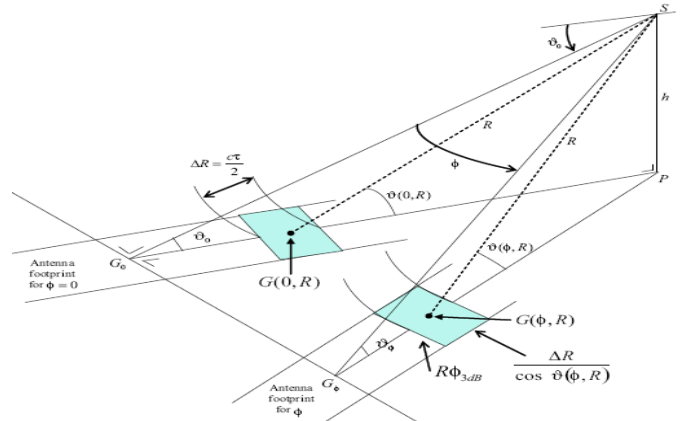


Fig.3. Imaging geometry for MMWR Imaging [1]

The patch formed by radar pulse is given by the intersection of the longitudinal wedge of width  $d_1$  with the transverse strip of width  $d_2$ . The area of intersection is given by,

$$A(\varphi, R) = d_1 d_2 = R \varphi_{3dB} \frac{\Delta R}{\cos \theta(\varphi, R)}$$

For a pulse width  $\tau$ , the range resolution is given by,

$$\Delta R = \frac{c\tau}{2}$$

The required information can be extracted by the measurement of received power  $P(\varphi, R)$  made by the radar as a continuous function of  $\varphi$  and  $R$  in real time. The following details supports the third requirement of the imaging sensor,

the measurement  $P(\phi, R)$  made by the radar is directly related to the power returned to the radar by the patch formed by  $A(\phi, R)$  [1]. The power returned by the patch  $A(\phi, R)$  is given by the radar equation as,

$$P(\phi, R) = \left[ \frac{P_t G^2 \lambda^2}{(4\pi)^3 R^4} \right] \sigma(\phi, R)$$

where,  $P_t$  is the transmitted power [W],  $G$  is the gain of the antenna in the direction of the patch,  $\lambda$  is the wavelength, and  $\sigma$  is the radar cross-section [ $m^2$ ] of the patch of interest, which varies with the location of the patch and thus with azimuth  $\phi$  and range  $R$ . Assuming that the patch is made of a single material,  $\sigma$  is given by,

$$\sigma(\phi, R) = \sigma_0(\phi, R)A(\phi, R)$$

Where,  $\sigma_0$  is the normalized cross-section (NRCS) [ $m^2/m^2$ ] of this material. Each type of material is characterized by a specific value of  $\sigma_0$ . Since the radar operates at small grazing angle, close to the slope of the flight path ( $\pm 3^\circ$ ), we assume that  $\theta(\phi, R) \approx \theta_\phi$  for all  $\phi$ 's. In addition, we operate at reasonably large values of  $R$  and within a limited range of values of  $\phi$  near  $\phi = 0^\circ$ . As a result, we also assume  $\theta_\phi \approx \theta_0$ . Of course, we can take into account all exact geometrical relations if desired, using above equations,

$$P(\phi, R) = \left[ \frac{P_t G^2 \lambda^2}{(4\pi)^3} \frac{c\tau}{2} \phi_{3dB} \right] \frac{\sigma_0(\phi, R)}{R^3 \cos \theta(\phi, R)} \approx \left[ \frac{P_t G^2 \lambda^2}{(4\pi)^3} \frac{c\tau}{2} \phi_{3dB} \right] \frac{\sigma_0(\phi, R)}{R^3 \cos \theta_0}$$

#### Effect of atmospheric attenuation on returned power

The above calculation of  $P(\phi, R)$  corresponds to the absence of any attenuation. In the presence of a real atmosphere, we take attenuation into account by multiplying  $P(\phi, R)$  by a factor  $e^{-0.2\alpha R}$  where  $\alpha$  is the appropriate one-way absorption (or attenuation) coefficient, generally given in units of dB/km. One model for attenuation by fog gives,

$$\alpha_f = \frac{0.438 M_w}{\lambda^2} \text{ [dB/km]}$$

Where,  $M_w$  is the mass of condensed water per unit volume of air (g/m<sup>3</sup>). This expression is reported to be accurate within 5% for  $\lambda$ 's between 2 and 10 cm. Another model for attenuation by fog gives,

$$\alpha_f = M_w \left( -1.347 + 0.372\lambda + \frac{18.0}{\lambda} - 0.022T \right)$$

This formula is reported valid for  $\lambda$ 's between 3 and 30 mm. The average value of  $M_w$  can be related to the optical visibility. One model for attenuation by rain gives

$$\alpha_r = 1.6 r^{0.64}$$

Where,  $r$  is the rainfall rate [mm/hr]. The final approximate expression for the power returned is,

$$P(\phi, R) = \left[ \frac{P_t G^2 \lambda^2}{(4\pi)^3} \frac{c\tau}{2} \phi_{3dB} \right] \frac{\sigma_0(\phi, R)}{R^3 \cos \theta_0} e^{-0.2\alpha R} \text{ [W]}$$

Returned power can be displayed either as B-scope image or on C-scope image [1] by mapping it to the scale of image intensities, typically from 0 to 255.

#### B-scope to C-scope conversion

When using radar to transit a dark rugged area, the pilot needs to recognize dangerous obstacles ahead from radar images. Since the radar image is displayed as range versus azimuth, the obstacles cannot be easily seen, and the heights of obstacles are especially difficult to determine. It is important to detect potential obstacles such as tall buildings so that the aircraft can avoid collision. Therefore, we investigated height reconstruction methods (including multi-scale wavelet and histogram analysis) on the extracted radar shadows formed by obstacles (see [8] for detailed height reconstruction methods). The height reconstruction result from B scope to C scope is shown in figure. 4.

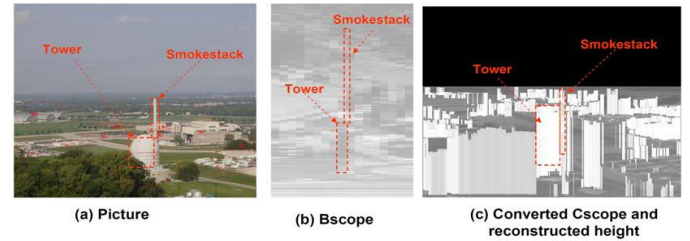


Fig.4. Reconstructed heights from B scope Radar image [8]

#### Backscattering Coefficient design (Normalised Radar Cross Section (NRCS) $\sigma_0$ )

The amount of the radiated energy is proportional to the target size, orientation, physical shape and material which are all lumped together in one target-specific parameter called Radar Cross Section (RCS) denoted by " $\sigma$ ". The radar cross section is defined as the ratio of the power reflected back to the radar to the power density incident on the target.

$$\sigma = \frac{P_r}{P_d} (m^2)$$

Where,  $P_d$  is power delivered to the radar signal processor by the antenna. Radar simulation involves the computation of a radar response based on the terrain's normalized radar cross section (NRCS). To compute normalized radar cross section for different types of terrain objects, we are using a well-known model called Phong like lighting model. Phong lighting is an empirically derived BRDF model for the computation of optical reflections [6]. The method is very popular in computer graphics and is broadly supported by different software and hardware platforms. Although the Phong lighting model is not physically correct since it does not obey all the laws of physics involved, it has easily interpretable parameters which may explain its popularity. Using the Phong model we compute the mean normalized radar cross section as,

$$\sigma = a \sin \theta + b \sin^c \theta$$

Where  $a$ ,  $b$  and  $c$  are the model parameters,  $a$  controls the amount of diffuse reflection of a material,  $b$  is the specular reflection coefficient and  $c$  is the specularity, that is, the sharpness of the directional highlight for a material (see [6] for more details about terrain types and  $a$ ,  $b$  and  $c$  values).

### Antenna gain ( $G$ )

The antenna gain of the radar is a known value. This is a measure of the antenna's ability to focus outgoing energy into the directed beam.

$$G = \frac{\text{Maximum radiation intensity}}{\text{Average radiation intensity}}$$

Antenna gain describes the degree to which an antenna concentrates electromagnetic energy in a narrow angular beam. The two parameters associated with the gain of an antenna are the directive gain and directivity. The gain of an antenna serves as a figure of merit relative to an isotropic source with the directivity of an isotropic antenna being equal to 1. The power received from a given target is directly related to the square of the antenna gain, while the antenna is used both for transmitting and receiving.

- The antenna gain increases the transmitted power in one desired direction.
- The reference is an isotropic antenna, which equally transmits in any arbitrary direction.

Power gain is determined by both the antenna pattern and by losses in the antenna. A useful rule of thumb for a typical antenna is,

$$G = \frac{26000}{(\theta, \phi)} \quad \theta \text{ and } \phi \text{ are elevation and azimuth angles in degrees respectively.}$$

### Range resolution

Range resolution is the ability of a radar system to distinguish between two or more targets on the same bearing but at different ranges. The degree of range resolution depends on the width of the transmitted pulse, the types and sizes of targets, and the efficiency of the receiver and indicator. Pulse width is the primary factor in range resolution. A well-designed radar system, with all other factors at maximum efficiency, should be able to distinguish targets separated by one-half the pulse width time. Therefore, the theoretical range resolution of a radar system can be calculated from the following formula.

$$\Delta R = \frac{c\tau}{2}, \text{ Where } \tau \text{ is pulse width.}$$

### Minimum detectable signal

In most cases optimal performance of a radar system can be obtained using the technique of *threshold detection*. In this method, the magnitude of each complex sample of the radar echo signal, possibly after signal conditioning and interference suppression is compared to a pre-computed threshold. If the

signal amplitude is below the threshold, it is assumed to be due to interference signals only. If it is above the threshold, it is assumed that the stronger signal is due to the presence of a target echo in addition to the interference, and a detection or "hit" is declared. In essence, the detector makes a decision as to whether the energy in each received signal sample is too large to likely have resulted from interference alone. If so, it is assumed a target echo contributed to that sample. Figure 5 illustrates the concept (see [7, 9] for equations and more details).

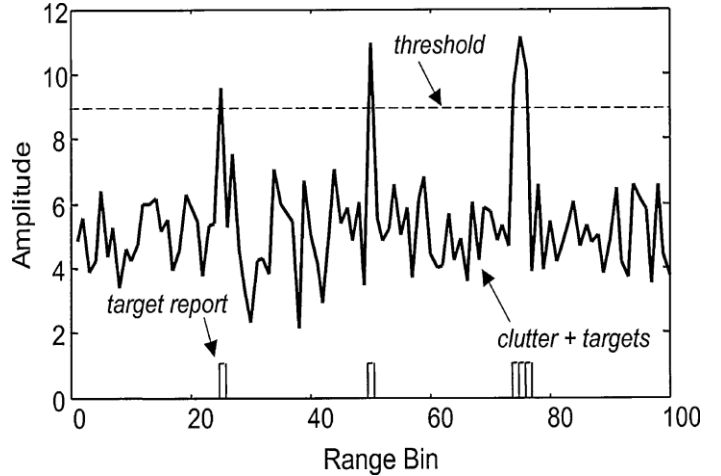


Fig.5. Illustration of threshold detection [7]

### III. SUMMARY OF MODELING PARAMETERS

With the help of all the above discussed details, the various modelling parameters are summarized as follows.

Waveform	FMCW (frequency modulated continuous wave)
Scanning principle	Frequency scanning
Centre Frequency	35 (GHz)
Wavelength	0.008571 (Meter)
Tau	0.5e-6 (Second)
Transmit power (Pt)	1 (Watt)
Azimuth field of view	41 (Degree)
Azimuth Beamwidth	0.8 (Degree)
Elevation Field of View	10 (Degree)
Range min	200 (Meter)
Range Limit	3500 (Meter)
Range max	Range min + Range Limit (Meter)
Range Resolution	6.67 (Meter/Pixel)
Azimuth Resolution	0.25 (Degree/Pixel)
Frame Rate	16 (Frames/second)
Elevation Max	28 (Degree)
Elevation Min	Elevation Max - Elevation Field of View
MROWS	floor(Range Limit/Range Resolution)
NCOLS	floor(Azimuth Field of View/Azimuth Resolution)
Elevation Resolution	Elevation Field of View/MROWS
Alpha	0 (1/meter)
C	3*10 <sup>8</sup> (Meter/Second)

Gain	26000/(Azimuth Beamwidth*Elevation Min)
Constant Power	$(Pt * Gain^2 * Wavelength^2 * c * \tau * (Azimuth \text{ Beamwidth} * \pi / 180)) / ((4 * \pi)^3 * 2 * \cos d \text{ (Elevation Min)})$
Antenna size	86*15*30 (centimeter <sup>3</sup> )
Weight	approximately 15kg

Table 2: Specifications of HiVision MilliMeter Wave Radar EVS sensor

To compute minimum detectable signal power

$$\text{Signal Min} = \text{Constant Power} * (1. / (\text{Range max.}^3));$$

To compute max possible received signal power

$$\text{Signal Max} = \text{Constant Power} * (1. / (\text{Range min.}^3));$$

Image Mapping Parameters

Intensity Min =0

Intensity Max =255

#### IV. CONCLUSION

New imaging sensors have a great impact on the design of the human machine interface of novel cockpit systems. These imaging sensors are responsible for the improvement of aircraft safety and operational qualities under adverse weather conditions. Hence, Procedure described in this paper that can provide the base for HiVision MilliMeter wave radar design, which is well suited for Enhanced Vision Systems applications.

#### ACKNOWLEDGMENT

All this work has been possible due to the well guided efforts and whole hearted support and encouragement of my external guide **Dr. Sudesh Kumar Kashyap**, Principal Scientist, Multi Sensor Data Fusion Group, Flight Mechanics & Control Division at National Aerospace Laboratories, Bangalore. Gratitude is also owed to our project head **Dr. N. Shantha Kumar** for his guidance and cooperation provided. I would like to thank **Dr. T V Rama Murthy**, Department of Electronics and Communication Engineering my internal guide for his invaluable suggestions.

#### REFERENCES

- [1] Maxime E. Bonjeana, Fabian D. Lapiereb, Jens Schiefelec, Jacques G. Verly, *Flight Simulator with IR and MMW Radar Image Generation Capabilities*, Proc of SPIE, Volume 6226, pp 62260A 8-12, April 2006.
- [2] Bemd Korn, Hans-Ullrich Doehler, and Peter Hecker, Institute of Flight Guidance, "*Weather Independent Flight Guidance: Analysis of MMW Radar Images for Approach and Landing*", 0-7695-0750-6/00 IEEE trans 2000
- [3] B. Korn, H.-U. Doehler and P. Hecker. "*MMW radar data processing for enhanced vision*". In J. G. Verly, editor, *Enhanced and Synthetic Vision 1999*, volume 3691, pages 29-38. SPIE, Apr. 1999.
- [4] H.U.Dohler, P.Hecker, R.Rodolff, "*Image data fusion for future Enhanced Vision Systems* "; *Sensor Data Fusion and Integration of the Human Element, system Concepts and Integration (SCI) Symposium*, Ottawa, 14-17 sep. 98, RTO Meeting Proceedings 12
- [5] H.-U. Doehler, T. Lueken, R. Lantzsche, "*ALL Flight - A full scale enhanced and synthetic vision sensor suite for helicopter applications*", *Enhanced and Synthetic Vision 2009*, edited by Jeff J. Güell, Maarten Uijt de Haag, Proc. Of SPIE Vol. 7328, 73280F. 2009 SPIE.
- [6] Niklas Peinecke, Hans-Ullrich Doehler, and Bernd R. Korn, "*Phong-like Lighting for MMW Radar Simulation*" Millimetre Wave and Terahertz

Sensors and Technology, edited by Keith A. Krapels, Neil A. Salmon, Proc. of SPIE Vol. 7117, 71170M · © 2008 SPIE

- [7] M.I. Skolnik, *Introduction to Radar Systems*, McGraw-Hill, NY, 1980.
- [8] Yunbao Huang, Xiaoping Qian, Brian Tsou "*Height Reconstruction from Radar Shadow*", from the report published in the interest of scientific and technical information exchange, Air Force Research Laboratory 711th Human Performance Wing USA , April 2009.
- [9] Ghulam Mehdi, Jungang Miao, "*Millimeter Wave FMCW Radar for Foreign Object Debris (FOD) Detection at Airport Runways*", *Proceedings of 2012 9th International Bhurban Conference on Applied Sciences & Technology (IBCAST) Islamabad, Pakistan, 9th - 12th January, 2012.*